HHS Public Access

Author manuscript

Curr Opin Chem Biol. Author manuscript; available in PMC 2016 August 01.

Published in final edited form as:

Curr Opin Chem Biol. 2015 August ; 27: 24–30. doi:10.1016/j.cbpa.2015.05.024.

Quantitative two-photon imaging of fluorescent biosensors

Gary Yellen and **Rebecca Mongeon**

Department of Neurobiology, Harvard Medical School, Boston, MA 02115

Abstract

Fluorescent biosensors are now routinely imaged using two-photon microscopy in intact tissue, for instance, in brain slices and brains in living animals. But most studies measure temporal variation – e.g., calcium transients in response to neuronal activity – rather than calibrated levels of biosensor occupancy (and thus levels of the sensed analyte). True quantitative measurements are challenging, since it is difficult or impossible to calibrate a sensor's dose-response *in situ*, and difficult to compare the optical signals from tissue to those during *in vitro* calibration. Ratiometric measurements (at two wavelengths) are complicated by variations in laser power and by wavelength-dependent attenuation in tissue. For some biosensors, fluorescence lifetime imaging microscopy (FLIM) provides a valuable alternative that gives well-calibrated measurements of analyte levels.

Graphical abstract

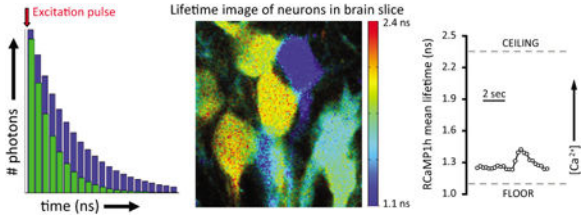

Introduction

Genetically encoded optical tools are providing fantastic new methods for manipulation and measurement of brain cells (and many others) in real time and with cellular specificity. Optical measurement gives a dramatic report of episodic activities: bursts of stimulus-triggered action potentials are brilliantly apparent as flashes in the fluorescence of highly optimized calcium sensors [1]. But for many important biological signals, a temporal pattern is not enough: a more intricate quantitative assessment of an optical reporter's signal is needed. And such quantitative measurement can be especially challenging in the context of brain imaging, both because the imaging involves two-photon excitation, and because the usual methods of signal calibration by chemical manipulation are difficult or impossible.

This review considers optimal approaches to quantitative biosensor imaging in this context, using either optical ratiometric or fluorescence lifetime imaging.

What is required for translating the fluorescent output of a biosensor into a quantitative measurement of the sensed level? A biosensor controlled by analyte binding[1] gives a fluorescent report that is proportional to its occupancy – the empty sensor usually has non-zero fluorescence, and the occupied sensor has a fluorescence that is greater or less than the empty value. But the intensity of any fluorescent signal will vary also with the concentration of the biosensor itself. To infer the occupancy of the sensor (and thus the concentration of analyte), the fluorescent signal must somehow be normalized to learn where it sits between the minimum and maximum values (Figure 1b). In some situations it is possible to measure these “floor” and “ceiling” values for each experiment – for instance, by permeabilizing the cells containing the biosensor and depleting or flooding the cell with the analyte. Ideally it is even possible to construct an *in situ* calibration curve for the sensor by observing the fluorescence response to known intermediate concentrations of the analyte.

Unfortunately, such *in situ* calibration is impossible when imaging the brain *in vivo*, and quite difficult even when imaging brain slices *in vitro*. Limited diffusional access combined with the cells' tendency to regulate the levels of all analytes of biological interest makes it impossible to control analyte concentration accurately.

The only alternative to *in situ* calibration is to use a calibrated optical measurement that can then be referred back to an *in vitro* calibration of optical response versus analyte concentration. The *in vitro* calibration would ideally be performed using protein samples or permeabilized cells viewed with the same microscope used for tissue imaging. Two imaging modalities can be used for this calibrated optical measurement: ratiometric imaging, and fluorescence lifetime imaging.

Ratiometric Two-Photon Imaging

The principle of ratiometric imaging is simple: fluorescence is measured at two different wavelengths. Analyte binding somehow changes the relative fluorescence at the two wavelengths, so that the ratio can be used to infer the level of analyte. The level of the biosensor itself will scale the two fluorescence values equally, so that there is no change in ratio.

Excitation-ratiometric biosensors

For fluorescent protein (FP) based sensors, one common type of ratiometric sensor is excitation ratiometric. The original green fluorescent protein (GFP) from jellyfish always emits green (~500-550 nm) light, but it has two excitation bands around 405 nm (A band) and 495 nm (B band) [2]. The “enhanced” GFP (EGFP) was cured of this problem – it has only the 495 nm excitation peak – but many GFP-based sensors exploit the two original GFP

[1]For simplicity, we focus our discussion on biosensors that bind a particular analyte and report its concentration; other types of sensors exist (for instance those that report on their own phosphorylation state and thus indirectly on protein kinase and protein phosphatase activity) that present additional problems in quantitation. We have also focused on genetically-encoded, fluorescent protein based sensors, though the same measurement principles apply to small molecule sensors.

bands for ratiometric sensing using a single circularly-permuted FP [3–5]. Binding of analyte shifts the resting state of the sensor between the two absorption bands, so that the relative response to the two excitation wavelengths is altered (Figure 1a,b). The switch between absorption bands can often be accomplished not only by analyte binding but also by environmental changes, particularly changes in pH. This is an important concern for the use of FP-based biosensors, requiring the simultaneous use of pH sensors for accurate calibration [6].

Excitation ratio measurements have long been used by biologists using standard one-photon excitation in the UV-visible range, particularly for the calcium-sensitive dyes such as the fura-2 dye introduced by Roger Tsien and colleagues in the 1980's [7]. As they described, the apparent affinity of the sensor varies systematically with the wavelengths chosen for the ratio measurement, and this important principle applies to all excitation-ratiometric measurements.

Each ratiometric image requires two separate exposures, using the two excitation wavelengths. For one-photon excitation, rapid wavelength switching can be accomplished using filter wheels, galvanometer-driven monochromators, or rapid switching of LED-based or laser light sources [34]. In the scanning two-photon microscope used for tissue and *in vivo* imaging, slow switching can be accomplished by tuning the pulsed excitation laser (typically a tunable Ti-sapphire laser) between two different excitation wavelengths. Even with modern integrated mode-locked lasers, tuning requires several seconds or more. Fast switching (on the millisecond time scale) requires a second (expensive) pulsed laser: each laser is tuned to a different excitation wavelength, and electronic shuttering (using electro-optical modulators) is used to allow sequential acquisition of signals evoked by the two lasers, often alternating by scan line [35].

An additional challenge for excitation ratio imaging with two-photon excitation is that two-photon excitation spectra often look very different from the one-photon spectra, because of the different rules for electronic transitions in response to one- vs. two-photon excitation [8]. Nevertheless, selective two-photon excitation of the A- and B-bands of GFP, and thus excitation-ratiometric measurement of FP biosensors, is possible [6,9–11] (Figure 1c).

Finally, how can excitation ratios be calibrated between different samples, and from time to time? Excitation ratios will be affected by variation in relative laser power at the two wavelengths. Wavelength-dependent scattering will also vary the effective excitation power with depth in the tissue: for instance, 800 nm light is scattered more than 950 nm light, so that an additional 100 micrometers depth in tissue will result in a ∼20% reduction in relative (800 nm / 900 nm) linear laser power, and thus a ∼30-40% reduction in two-photon excitation [calculations based on [12]].

Ideally, to correct for power fluctuation in laser output and depth-dependent variation, one would like an accurate report of the relative two-photon excitation power at the two excitation wavelengths, under the specific conditions of the experiment (imaging depth, actual laser power and pulse duration at the imaging site). The best calibration tool would be an FP that always produces the same relative response to A- and B-band excitation – which

would allow adjustment of the relative power or the relative output measurements. Failing this (as we are unaware of such an FP), we propose the use of a ratiometric FP such as pHluorin [13] to indicate relative power in the A- and B- bands, combined with an independent, fluorescence lifetime based measurement of the pH to control for the pH effect on the relative fluorescence of those bands [14,15][2].

Emission-ratiometric biosensors, including FRET sensors

A second ratiometric sensor design depends on Förster resonance energy transfer (FRET) between two FPs [16–20]. This energy transfer, for instance from a cyan FP to a yellow FP, depends on overlap between the emission band of one FP (the donor) and the excitation band of the second FP (the acceptor), as well as on the distance and orientation between the FPs. This principle has been used to report on the interaction between two separate proteins, each tagged with one FP [21]. For analyte-binding biosensors, the design allows analyte binding to change the relative position of the two FPs, and thus the efficiency of FRET. A variety of imaging strategies is used for such sensors (viz. [22–24]), but the simplest involves a straightforward emission ratio measurement. A single excitation wavelength is chosen, which selectively excites the short-wave donor FP. Depending on the analyte concentration, some of the donor FPs transfer their excited state energy to a neighboring acceptor FP by a non-radiative mechanism, while others do not. Therefore the ratio of donor emission to acceptor emission reflects the efficiency of FRET, which in turn reflects the analyte concentration. Corrections must be made for the overlap in both excitation and emission spectra: some acceptor FPs will be inadvertently excited directly[3], and some of the light emitted from donor FPs will be in the wavelength range used for detecting the acceptor emission.

Other non-FRET biosensors also can be monitored using an emission ratio. Some have been produced using single FPs [9,25,26], though single FP sensors are usually excitation ratiometric; others involve non-FRET intramolecular interactions of multiple FPs [27]. Sometimes single FP sensors that respond to analyte binding with an intensity change alone are combined in tandem with a second FP of a different color, to normalize for sensor concentration [28]. While this allows some degree of calibration, all dual FP sensors are subject to variation from prep to prep and time to time in the absolute emission ratio, because different FPs mature at different rates and also photobleach at different rates.

Emission ratios are somewhat more resistant than excitation ratios to wavelength-dependent attenuation in tissue. For instance, emission attenuation due to scattering alone is predicted to give about a 10% change in the ratio of green (525 nm) to red (625 nm) emission for a change of 100 um in depth[4]. In the case of blood-perfused brain tissue *in vivo*, however, hemoglobin absorbance increases the total depth-dependent change in emission ratio to about 30-40% for 100 um variation in depth[5].

---

[2]The relative fluorescence of the two absorption bands of FPs is often affected by pH; in pH reporters like pHluorin, this dependence is well-characterized.
[3]And this problem may be worse with two-photon excitation.
[4]The attenuation estimates in this paragraph were calculated by the authors using scattering and absorbance data from [29].
[5]We are unaware of attempts to correct for this color bias. In principle, it seems that fluorescent beads of various colors or tandem expression of non-biosensor FPs could be used to estimate the empirical magnitude of this depth-dependent effect and to correct it.

Fluorescence lifetime imaging

Compared with ratiometric approaches, fluorescence lifetime imaging microscopy (FLIM) provides a more robust imaging modality for quantitative biosensor imaging when imaging in tissue. Fluorescence lifetime is defined as the time between absorption of an "excitation photon" (or two photons), and the subsequent emission of a photon. As for a radioactive decay process, the emission of individual photons is stochastic, but the statistics of the decay process are characteristic of the fluorophore and describe the dwell time in the excited state (Figure 2a). For FP fluorescence, as for other chromophores, the dwell time in the excited state is determined by the total exit rate from the excited state. The excited state can return to the ground state not only by emission of a fluorescence photon, but also by non-radiative energy decay (quenching) or energy transfer (e.g. FRET).

Fluorescence biosensors often exhibit changes in fluorescence lifetime, in addition to their change in fluorescence intensity. For instance, when the fluorescence output of a single FP biosensor is increased by analyte binding, this may correspond to reduced quenching (perhaps because the β-barrel structure provides increased protection of the fluorophore from solvent) – in which case fluorescence lifetime will likely increase[6]. Several single FP sensors exhibit very substantial changes in fluorescence lifetime [15] (Figure 3)

Also, virtually all FRET sensors should exhibit a change in fluorescence lifetime of the donor FP (the cyan FP in our example before), since FRET provides an additional non-radiative decay pathway for the excited state of the donor FP [30][7]. When using fluorescence lifetime to monitor the state of a FRET biosensor, it becomes possible to use a completely non-fluorescent acceptor species [31]. This reduces the portion of the visible spectrum used for a single biosensor measurement, and allows simultaneous use of multiple sensors.

Fluorescence lifetime provides a very easy calibration between a biosensor measurement in tissue and the reference calibration of the sensor *in vitro*. Lifetime is an intensive rather than an extensive property of the fluorophore, so the measurement does not vary with the expression level of the biosensor. In contrast to the ratiometric methods, which involve measurements at multiple wavelengths and thus correction for the relative excitation power, attenuation, and filter efficiencies in the particular instrument used for the measurement, fluorescence lifetime is measured in well-calibrated units of time that can be referenced directly between different instruments.

The standard equipment of a two-photon microscope facilitates the measurement of fluorescence lifetime, because the pulsed laser needed for two-photon excitation provides a well-defined "start time" for determining fluorescence lifetime.. Time-correlated single

[6]Some single FP sensors, particularly those developed for ratiometric imaging, exhibit little or no change in fluorescence lifetime, however. In principle, analyte binding to a sensor can produce a change in absorbance, a change in quantum yield, or both. Only changes in quantum yield are seen as changes in lifetime. Ratiometric sensors are selected to have a large shift between A- and B-band absorbance, which itself produces no change in lifetime; but they may also have a change in quantum yield and thus lifetime. During sensor development it is possible to select versions that have substantial lifetime changes.

[7]We have found that some sensors that were designed to operate by a FRET mechanism do not exhibit any change in donor fluorescence lifetime [R.M. and G.Y., unpublished]. We conclude either that those sensors do not actually use a FRET mechanism (though they do exhibit a change in emission ratio between the FPs), or that in the non-FRET state there is some offsetting quenching process that depresses the donor lifetime equivalently to the FRET state.

photon counting (TCSPC) involves the measurement of the arrival time of each emitted photon, relative to the most recent laser pulse (which is the one most likely to have provoked the emission) (Figure 2b) [32]. Almost all lasers for two-photon microscopy operate with a repetition rate of ∼80 MHz, so the ∼12.5 ns between laser pulses allows an excellent measurement window for the exponential decay of the excited state, which for fluorescent proteins is typically in the 1-3 ns range.

The detection electronics for FLIM have been the tricky and expensive part of lifetime imaging. The traditional hybrid analog-digital systems have time-to-amplitude converters and digitizers that are limited by their electronic reset times – after detecting a photon, they are blind to additional photons for the next 100-125 ns [32]. Additionally, the photon arrival time measurements become biased if two photons arrive in response to the same laser pulse. Both of these issues (referred to as “dead time” and “pile-up”, respectively) limit the incident photon intensity and thus limit dynamic range and prolong data collection times; they also affect the accuracy of the lifetime measurement.

These problems can be overcome by a fully digitized detection system. State-of-the-art digitizers can convert analog signals to digital values at rates exceeding one value per nanosecond (gigasamples per second). While no ordinary sequential microprocessor is capable of processing photon detector signals at this rate, parallel and pipelined processing based on field-programmable gate array (FPGA) technology permits the continuous processing of photon detector signals into fluorescence lifetime images (G.Y., unpublished). This digitized FLIM approach has no “dead time” issues and is able to avoid “pile-up” by excluding multiple photon events from analysis (though such multiple photon events are counted for intensity purposes). Such a digitized FLIM system is capable of imaging a wide dynamic range of light (with a maximum lifetime count rate of ∼30 MHz obtained when the mean photon rate is one per laser pulse, i.e. ∼80 MHz, based on Poisson statistics).

All FLIM systems collect fluorescence decay curves (Figure 2, Figure 3a) that are then fit with multiple-exponential functions to define the contribution of different lifetime components. This detailed fitting is important particularly when the fluorescence signal is contributed by multiple fluorophores [32,33]. But for biosensor imaging, most of the collected light comes from a single known fluorophore, the biosensor itself[8]. Once a biosensor's lifetime over a range of analyte concentrations has been measured, detailed fitting is no longer required – the occupancy state can be inferred from simple parametric measurements of lifetime – such as the mean empirical lifetime[9] (Figure 3). This allows usable lifetime data, with mean lifetime error on the order of 1%, to be collected in less than a second, or even in milliseconds with a focused scan (e.g. a line scan) and with bright samples[10].

[8]When biosensor expression is low, tissue autofluorescence may become a confounding factor both for lifetime measurement and ratiometric measurement.

[9]Also referred to as mean arrival time or the first moment of the lifetime distribution [32].

[10]The number of photons required within a region of interest (ROI) to achieve a 1% standard error in the lifetime measurement is ∼10,000 (based on sampling error ∼ 1/√N). At moderate photon fluxes of 1 - 5 MHz, this would require an ROI sample time of ∼2 - 10 ms. For a full frame large enough to accommodate ∼25 such ROIs, the practical full-frame acquisition time would be ∼0.1 – 0.4 sec.

As an imaging modality for fluorescent biosensors, FLIM thus offers a very valuable and much more readily calibrated alternative to ratiometric measurements when quantitative imaging is the goal.

Acknowledgments

We are grateful for support from NIH (DP1 EB016985 and R01 NS055031 to G.Y., F32 NS080455 to R.M.) and the David Mahoney Fellowship (to R.M.).

References

1. Chen TW, Wardill TJ, Sun Y, Pulver SR, Renninger SL, Baohan A, Schreiter ER, Kerr RA, Orger MB, Jayaraman V, et al. Ultrasensitive fluorescent proteins for imaging neuronal activity. Nature. 2013; 499:295–300. [PubMed: 23868258]
2. Tsien RY. The green fluorescent protein. Annu Rev Biochem. 1998; 67:509–544. [PubMed: 9759496]
3. Nagai T, Sawano A, Park ES, Miyawaki A. Circularly permuted green fluorescent proteins engineered to sense Ca^{2+} Proc Natl Acad Sci. 2001; 98:3197–3202. [PubMed: 11248055]
4. Belousov VV, Fradkov AF, Lukyanov KA, Staroverov DB, Shakhbazov KS, Terskikh AV, Lukyanov S. Genetically encoded fluorescent indicator for intracellular hydrogen peroxide. Nat Methods. 2006; 3:281–286. [PubMed: 16554833]
5. Berg J, Hung YP, Yellen G. A genetically encoded fluorescent reporter of ATP:ADP ratio. Nat Methods. 2009; 6:161–166. [PubMed: 19122669]
6. Tantama M, Martínez-François JR, Mongeon R, Yellen G. Imaging energy status in live cells with a fluorescent biosensor of the intracellular ATP-to-ADP ratio. Nat Commun. 2013; 4:2550. [PubMed: 24096541]
7. Grynkiewicz G, Poenie M, Tsien RY. A new generation of Ca^{2+} indicators with greatly improved fluorescence properties. J Biol Chem. 1985; 260:3440–3450. [PubMed: 3838314]
8. Drobizhev M, Makarov NS, Tillo SE, Hughes TE, Rebane A. Two-photon absorption properties of fluorescent proteins. Nat Methods. 2011; 8:393–399. [PubMed: 21527931]
9. Bizzarri R, Serresi M, Luin S, Beltram F. Green fluorescent protein based pH indicators for in vivo use: a review. Anal Bioanal Chem. 2008; 393:1107–1122. [PubMed: 19034433]
10*. Akerboom J, Carreras Calderón N, Tian L, Wabnig S, Prigge M, Tolö J, Gordus A, Orger MB, Severi KE, Macklin JJ, et al. Genetically encoded calcium indicators for multicolor neural activity imaging and combination with optogenetics. Front Mol Neurosci. 2013; 6:2. Reports new color variants of the widely-used GCaMP calcium sensor. The yellow YCaMP1b is shown to be excitation ratiometric for 2-photon measurements. The red RCaMP1h is not ratiometric, but it exhibits a substantial difference in fluorescence lifetime (shown in this review, Figure 3). [PubMed: 23459413]
11*. Breckwoldt MO, Pfister FMJ, Bradley PM, Marinković P, Williams PR, Brill MS, Plomer B, Schmalz A, St Clair DK, Naumann R, et al. Multiparametric optical analysis of mitochondrial redox signals during neuronal physiology and pathology in vivo. Nat Med. 2014; 20:555–560. Uses multiple imaging modalities to measure mitochondrial pH and redox as well as morphology. Includes two-photon excitation ratiometric measurements, by laser tuning, on the genetically encoded redox sensor mito-Grx1-roGFP2. [PubMed: 24747747]
12. Horton NG, Wang K, Kobat D, Clark CG, Wise FW, Schaffer CB, Xu C. In vivo three-photon microscopy of subcortical structures within an intact mouse brain. Nat Photonics. 2013; 7:205–209.
13. Miesenböck G, De Angelis DA, Rothman JE. Visualizing secretion and synaptic transmission with pH-sensitive green fluorescent proteins. Nature. 1998; 394:192–195. [PubMed: 9671304]
14. Szmacinski H, Lakowicz JR. Optical measurements of pH using fluorescence lifetimes and phase-modulation fluorometry. Anal Chem. 1993; 65:1668–1674. [PubMed: 8368522]

15. Tantama M, Hung YP, Yellen G. Imaging intracellular pH in live cells with a genetically encoded red fluorescent protein sensor. J Am Chem Soc. 2011; 133:10034–10037. [PubMed: 21631110]

16. Selvin PR. Fluorescence resonance energy transfer. Methods Enzymol. 1995; 246:300–334. [PubMed: 7752929]

17. Miyawaki A, Griesbeck O, Heim R, Tsien RY. Dynamic and quantitative Ca^{2+} measurements using improved cameleons. Proc Natl Acad Sci. 1999; 96:2135–2140. [PubMed: 10051607]

18. Miyawaki A, Llopis J, Heim R, McCaffery JM, Adams JA, Ikura M, Tsien RY. Fluorescent indicators for Ca^{2+} based on green fluorescent proteins and calmodulin. Nature. 1997; 388:882–887. [PubMed: 9278050]

19. Deuschle K, Okumoto S, Fehr M, Looger LL, Kozhukh L, Frommer WB. Construction and optimization of a family of genetically encoded metabolite sensors by semirational protein engineering. Protein Sci Publ Protein Soc. 2005; 14:2304–2314.

20. Duebel J, Haverkamp S, Schleich W, Feng G, Augustine GJ, Kuner T, Euler T. Two-photon imaging reveals somatodendritic chloride gradient in retinal ON-type bipolar cells expressing the biosensor Clomeleon. Neuron. 2006; 49:81–94. [PubMed: 16387641]

21. Yasuda R. Imaging intracellular signaling using two-photon fluorescent lifetime imaging microscopy. Cold Spring Harb Protoc. 2012; 2012:1121–1128. [PubMed: 23118363]

22. Erickson MG, Alseikhan BA, Peterson BZ, Yue DT. Preassociation of calmodulin with voltage-gated Ca^{2+} channels revealed by FRET in single living cells. Neuron. 2001; 31:973–985. [PubMed: 11580897]

23. Tadross MR, Park SA, Veeramani B, Yue DT. Robust approaches to quantitative ratiometric FRET imaging of CFP/YFP fluorophores under confocal microscopy. J Microsc. 2009; 233:192–204. [PubMed: 19196425]

24. Piston DW, Kremers GJ. Fluorescent protein FRET: the good, the bad and the ugly. Trends Biochem Sci. 2007; 32:407–414. [PubMed: 17764955]

25. Hanson GT, McAnaney TB, Park ES, Rendell MEP, Yarbrough DK, Chu S, Xi L, Boxer SG, Montrose MH, Remington SJ. Green fluorescent protein variants as ratiometric dual emission pH sensors. 1. Structural characterization and preliminary application. Biochemistry. 2002; 41:15477–15488. [PubMed: 12501176]

26. Zhao Y, Araki S, Wu J, Teramoto T, Chang YF, Nakano M, Abdelfattah AS, Fujiwara M, Ishihara T, Nagai T, et al. An expanded palette of genetically encoded Ca^{2+} indicators. Science. 2011; 333:1888–1891. [PubMed: 21903779]

27*. Ding Y, Li J, Enterina JR, Shen Y, Zhang I, Tewson PH, Mo GCH, Zhang J, Quinn AM, Hughes TE, et al. Ratiometric biosensors based on dimerization-dependent fluorescent protein exchange. Nat Methods. 2015; 12:195–198. Describes the construction of emission-ratiometric sensors using a novel design, in which analyte binding (or caspase cleavage) change the intramolecular association between a nonfluorescent enhancer FP and either a red or a green dimerization-dependent FP. [PubMed: 25622108]

28. Hung YP, Albeck JG, Tantama M, Yellen G. Imaging cytosolic NADH-NAD^+ redox state with a genetically encoded fluorescent biosensor. Cell Metab. 2011; 14:545–554. [PubMed: 21982714]

29. Jacques SL. Optical properties of biological tissues: a review. Phys Med Biol. 2013; 58:R37. [PubMed: 23666068]

30. Chen Y, Saulnier JL, Yellen G, Sabatini BL. A PKA activity sensor for quantitative analysis of endogenous GPCR signaling via 2-photon FRET-FLIM imaging. Front Pharmacol. 2014; 5:56. [PubMed: 24765076]

31. Murakoshi H, Lee SJ, Yasuda R. Highly sensitive and quantitative FRET-FLIM imaging in single dendritic spines using improved non-radiative YFP. Brain Cell Biol. 2008; 36:31–42. [PubMed: 18512154]

32*. Becker, W. The bh TCSPC handbook. Becker & Hickl GmbH; 2014. A comprehensive explanation of the principles and practical measurement of fluorescence lifetime by time-correlated single photon counting (TCSPC)

33. Rice WL, Shcherbakova DM, Verkhusha VV, Kumar ATN. In vivo tomographic imaging of deep seated cancer using fluorescence lifetime contrast. Cancer Res. 201510.1158/0008-5472.CAN-14-3001

34. Shimozono S, Fukano T, Nagai T, Kirino Y, Mizuno H, Miyawaki A. Confocal imaging of subcellular Ca^{2+} concentrations using a dual-excitation ratiometric indicator based on green fluorescent protein. Sci STKE. 2002; 2002(125):l4.

35. Ding JB, Takasaki KT, Sabatini BL. Supraresolution imaging in brain slices using stimulated-emission depletion two-photon laser scanning microscopy. Neuron. 2009; 63:429–37. [PubMed: 19709626]

36. Hosoi H, Yamaguchi S, Mizuno H, Miyawaki A, Tahara T. Hidden electronic excited state of enhanced green fluorescent protein. J Phys Chem B. 2008; 112:2761–3. [PubMed: 18275187]

Highlights

- Two-photon imaging of biosensors in intact tissue is challenging to calibrate.
- Ratiometric or fluorescence lifetime imaging can provide the needed normalization.
- Calibrated ratiometric imaging requires depth and power correction.
- Fluorescence lifetime imaging provides a calibrated readout of sensor occupancy.

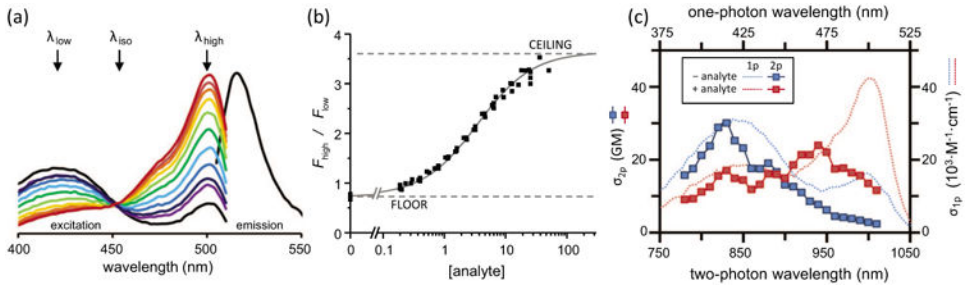

Figure 1.

Fluorescence behavior of a ratiometric biosensor. The examples here are for an ATP sensor, PercevalHR (adapted from [6]). **(a)** An excitation ratiometric sensor changes its excitation spectrum as analyte concentration is increased (from black to red). Relative fluorescence increases at some wavelengths (λ_{high}), decreases at others (λ_{low}), and often exhibits an isosbestic wavelength where there is no change (λ_{iso}). **(b)** The ratio varies predictably as a function of analyte concentration. **(c)** Comparison of the excitation spectra for one-photon and two-photon excitation, with and without analyte. The energy of a single photon of wavelength 425 nm is equivalent to the energy of two photons at 850 nm, but the two-photon excitation spectrum is not quite predictable from the single-photon excitation spectrum. Nevertheless, it is possible for this excitation-ratiometric sensor to be ratio-imaged using two-photon excitation (e.g. at 950 and 830 nm; see also [36]).

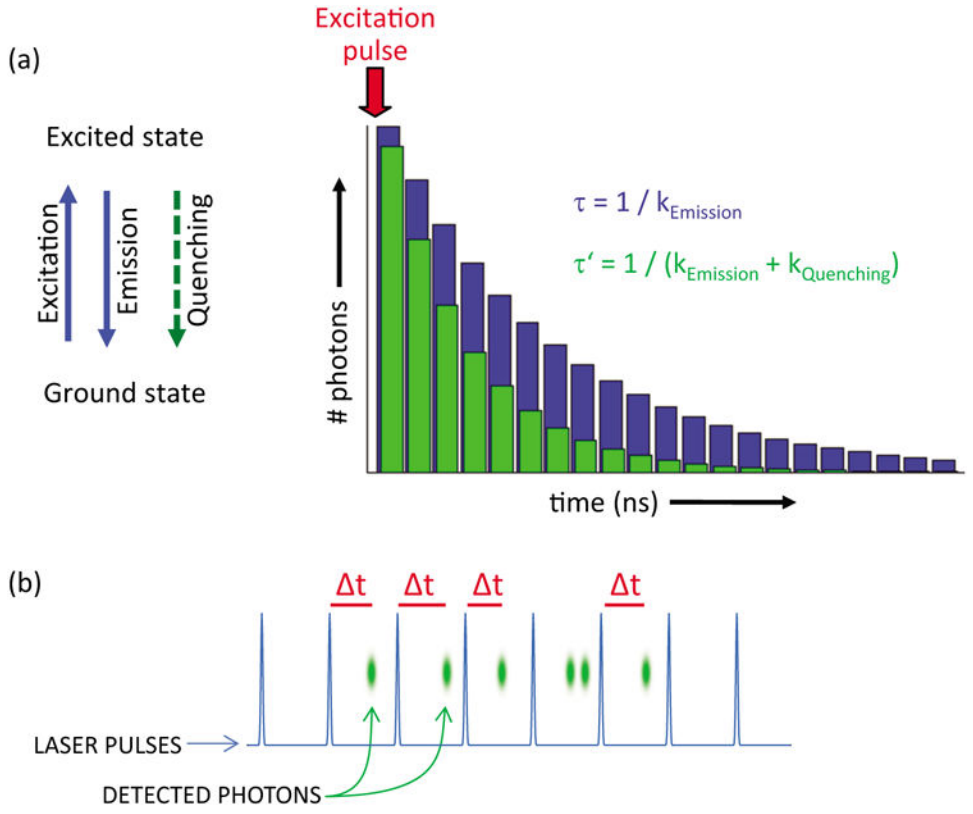

Figure 2.

Fluorescence lifetime: theory and measurement. **(a)** Fluorescence lifetime reports the average dwell time of a fluorophore in the excited state. After excitation, a photon is emitted at a random time, whose average value τ is inversely related to the rate constant for emission. If a non-radiative "quenching" rate is added, the average dwell time in the excited state is reduced. **(b)** Time-correlated single photon counting with a pulsed laser source. The two-photon excitation laser fires continuously at ~80 MHz, or once every 12.5 ns (the actual pulse duration is exaggerated in the diagram; a typical pulse duration is only 0.0001 ns). Whenever only a single photon is detected after a laser pulse, the time delay (Δt) is measured from the laser pulse to the photon detection. Depending on the average photon flux, some laser pulses will elicit no fluorescence, some will have single photons, and some will have more than one photon (which makes a precise delay measurement impossible). A histogram of many Δt values gives an exponential decay plot like that in (a); these are often plotted with a logarithmic y-axis, which makes a single exponential appear like a straight line. An arithmetic average of the Δt values gives an "empirical mean τ" value, and the standard error of this mean value is related to $(N_{photons})^{-1/2}$.

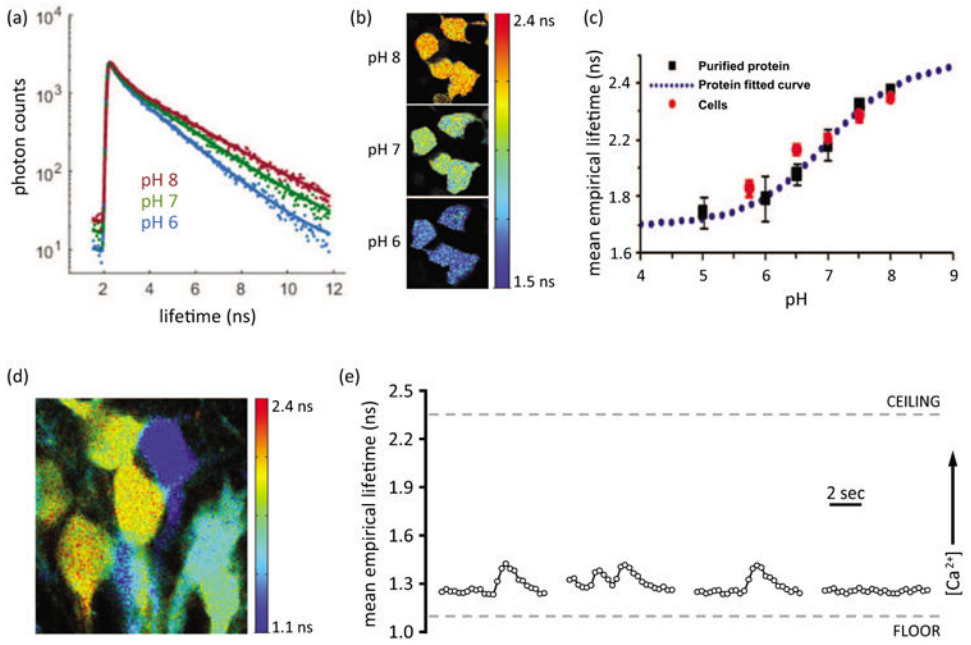

Figure 3.

Fluorescence lifetime imaging: cellular pH determination and calcium dynamics. **(a)** Lifetime decay curves of pHRed sensor fluorescence in HEK293 cells clamped at an intracellular pH of 6, 7 and 8 (nigericin method, [15]). Each decay curve is well described by a biexponential fit (shown) with average τ decay values of 1.66, 1.96 and 2.17 ns for pH 6, 7 and 8, respectively. **(b)** Fluorescence lifetime images of the HEK293 cells used to generate the decay curves in (a). Pixels are pseudo-colored according to the mean empirical lifetime, a fit-free parametric measurement. The mean empirical lifetime values are 1.65, 1.97 and 2.19 ns for cells at pH 6, 7 and 8, respectively. The mean empirical lifetime corresponds well to the fitted average τ values at each pH. **(c)** Calibration of the fluorescence lifetime response of pHRed to pH changes (adapted from [15]). **(d)** Fluorescence lifetime image of hippocampal dentate granule neurons in a brain slice preparation expressing the RCaMP1h calcium sensor [10]. Spontaneous electrical activity and calcium responses were elicited by addition of 7.5 mM extracellular KCl. The pseudo-colored image shown indicates the fluorescence lifetime of each neuron averaged over approximately 5 seconds. **(e)** Sub-second changes in RCaMP1h fluorescence due to cellular calcium dynamics are easily resolved using lifetime imaging. Mean empirical fluorescence lifetime is plotted for each 266 ms frame (black circles in traces), imaging the sensor in a single dentate granule neuron. Four separate episodes of spontaneous activity are illustrated. Maximum and minimum observed lifetime values for RCaMP1h are indicated as ceiling and floor, respectively; in principle the calibration of fluorescence lifetime of RCaMP1h to calcium concentration can be accomplished similarly to that shown in (c) for pHRed sensor. The photon flux of ~0.5 MHz and total photon counts of ~30,000 photons yielded <0.6% error in the mean lifetime estimation.